

DISTRIBUTION STATEMENT A

Approved for Public Release

Distribution Unlimited

LIFING AND LIFE EXTENSION OF FRACTURE CRITICAL AEROENGINE COMPONENTS

A.D. Boyd-Lee, G.F. Harrison* and D. Painter,

Mechanical Sciences Sector (MSS), Defence Evaluation and Research Agency (DERA),
Farnborough, Hampshire, GU14 0LX, UK

Abstract

Engine removal costs and the consequences of grounding aircraft are many times greater than the replacement component costs. The paper addresses several areas where DERA has been instrumental in generating procedures to enable more of the available safe service lives of fracture critical aeroengine components to be utilised. More effective methods for handling non-finite results (discontinued fatigue tests) are explored. General life extension via support of the '2/3 dysfunction' is considered and also the associated procedures necessary for 'cashing in' any available safe crack growth life beyond life-to-first-crack. The paper addresses the development of robust risk management procedures for situations where operational requirements demand the short-term continued use of life expired parts. Finally, some results of short crack growth modelling aimed at enhanced lifing methods are presented.

Nomenclature

	given that:
β	mission exchange rate
\prod	product of a series of terms
σ	population standard deviation
Ar	declared safe service life (reference cycles)
Efh	engine flying hours
GM	Geometric Mean
H	component life
n	sample size
N	fatigue life (reference cycles)
p(x)	probability of event x
PD(x)	probability density function w.r.t. x
S	safety factor

Subscripts and superscripts

'	implies a change of variable
-	refers to non-finite value
μ	refers to geometric mean value
b	refers to burst distribution
i	refers to LTFC value
ref	refers to reference load

*: Professor.

© Crown Copyright 1999/DERA

Published with the permission of HMSO

Introduction

Aeroengine gas-turbine components operate in extremely hostile environments and over a range of complex thermo-mechanical loading conditions. A consequence of the drive for improved thrust and lower fuel consumption is that each stage in the engine is required to do more work, more efficiently. This means fewer, more heavily loaded stages and trade-off studies are carried out to optimise the design within the constraints of the performance, weight and cost target specifications. Component integrity is the overriding requirement in engine certification and safe service operation and before any life extension scheme can be introduced, it must be demonstrated that airworthiness will not be compromised. The major fracture-critical components are identified as the turbine and compressor discs and shafts, since their failure in service could be hazardous to the safety of the aircraft and its occupants.

Life-to-first-crack

Under current UK Military Defence Standards (Def. Stan. 00-971)¹ and European Civil Joint Airworthiness Requirements (JAR-E)², the service lives for fracture-critical components are derived from spin-rig test results of actual engine discs under cyclic loading at stress and temperature conditions similar to those experienced in engine operation. These regulations are based on a safe-life policy wherein component fatigue 'failure' is defined as the occurrence of an 'engineering crack' of 0.38mm radius.

With each test costing in the region of £100,000, the number of available results is usually small. The lifing regulations define the procedure for the safe interpretation of these results and for calculation of the declared safe service lives. That is, a predicted safe cyclic life (PSCL) is calculated by applying statistically-derived safety factors to the geometric mean (GM) of the respective test results, such that at this life, not more than 1 in 750 service discs would be expected to contain an 'engineering crack', to 95% confidence. It is from this base that the life-extension procedures discussed in the paper are quantitatively assessed.

Experience has shown that disc fatigue lives are distributed according to a lognormal density function, to a good approximation. Also a conservative assumption is made that the ratio of the fatigue lives at

20000208 065

the $+3\sigma$ and -3σ points on the life-to-first-crack (LTFC) distributions is 6, which has wide applicability to aeroengine disc materials. Given an assumed scatter factor of 6, the life corresponding to the lower 1/750 quantile is automatically located at a factor of $\sqrt[6]{6}$ ($= 2.449$) below the geometric mean (GM) LTFC obtained from the sample.

The 95% confidence level allows for the effect of component test sampling error on the safety level inherent in the calculation. This lower confidence bound corresponds to a safety factor in life of:

$$6 \left(\frac{1.645}{6\sqrt{n}} \right) \quad (1)$$

where the 95% confidence corresponds to 1.645 standard deviations. It can be seen that equation 1 is an increasing function with respect to decreasing sample size. In summary, a predicted safe cyclic life (PSCL) or Ar is calculated by an equation of the type:

$$Ar = \frac{\sqrt[n]{\prod_{i=1}^n N_i}}{2.449 \times 6 \left(\frac{1.645}{6\sqrt{n}} \right)} \quad (2)$$

where 'N_i' are the individual LTFC test results. Application of factors involved in determining 'Ar' is illustrated in figure 1.

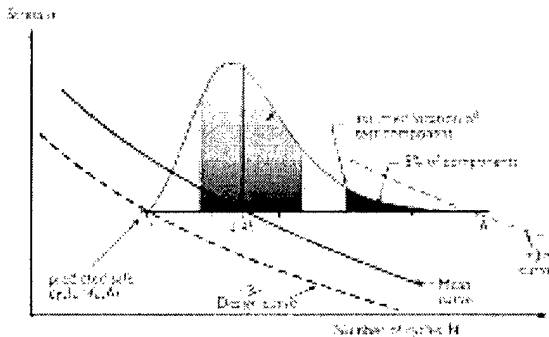


Figure 1. Derivation of the material design curve and predicted safe cyclic life.

Through using an 'engineering crack' as the basis for the calculation, the additional life taken to grow to the critical size associated with dysfunction (failure) acts as a further margin of safety. Ultimately, it is this, in combination with the factors in the denominator of equation 2 which define the actual safety level inherent in the application of this method. A final safety feature is that when a new design of component enters service, a release life of only 50% of its PSCL is approved. When the lead disc reaches this life, it is withdrawn for spin testing, whilst the other discs are allowed to remain in service for up to 75% PSCL. The ex-service disc test result is added to the sample and the component life revised accordingly. After a second ex-service disc test, the remaining discs are allowed to remain in service for the full 100% PSCL, the life now being identified as 'Ar.'

Life revision of in-service components

A consequence of the high cost of disc spinning tests is that once a specified (required) design life has been demonstrated, there is great pressure to discontinue the respective test programme, even though the discs have not reached 'failure' (defined as the occurrence of an engineering crack). Results of this kind are called 'non-finite'. Non-finite results can also arise for several other reasons. Amongst these, a common cause is a change in the identified failure location within a component as the result of either service experience or reanalysis of the basic design.

The current lifing regulations were originally derived to accept only finite results and this has caused non-finite results to be either rejected unnecessarily or accepted overconservatively by assuming 'failure on the next load cycle'. The corollary is, that where the newly established failure location is now identified as having experienced little or no overstress, the service life that can now be declared would need to be reduced by a factor of up to 4, depending on the number of test results available. Under this approach, where for illustration, a sample of 5 tests were conducted at a typical overstress of level of '1.1' and each was discontinued after 10,000 cycles, then application of equation 2 would allow a life of 5,422 cycles to be declared. If subsequently, the failure was determined to occur at a different critical location, but which, also typical of standard tests had no overstress, then under current regulations, each of these 10,000 cycle non-finite results would require to be treated as finite with a life of 10,001 cycles. This would allow a service life of only 3,277 cycles to be declared, thus enforcing a 40% service life reduction. Methods proposed to alleviate this problem are discussed in the next section.

Life extension via the exploitation of non-finite fatigue test results

Favourable sub-sample

One approach, approved in current regulations, is to ignore unfavourable non-finite results and assume 'failure on the next cycle' for the remaining non-finite results. This removes the penalty of having to assume that a relatively short non-finite result will fail in the next cycle. In general, this method is still overconservative, since low non-finite values do not indicate that the corresponding finite values are also low.

Rank order

Another approximate method is to 'rank order' the results and plot them on cumulative probability paper. This method has some merit for mixed finite and non-finite results. Indeed, for a reasonable sample size, where the non-finite results form less than 50% of the sample and all are long life discontinued tests, much less error is introduced than by the selection of a favourable sub-sample. However, larger errors can occur when it is not possible to rank order the finite and non-finite results in a given sample. For example, the rank order of a non-finite result of 10,000 cycles and a finite result of 12,000 cycles is indeterminate.

Improved statistical analysis of non-finite results

This subsection presents an analysis methodology for samples comprised of only non-finite results, for illustration. The general methodology can also handle samples comprised of mixed finite and non-finite data, and has been applied to a variety of distributions. As a further simplification, the following analysis is restricted to samples that can be assumed to belong to a lognormal LTFC distribution having a known scatter factor.

No significant results are rejected by the improved approach. As is the case for samples of finite results: i) the geometric mean (GM) of the population LTFC distribution is estimated to 95% confidence, and ii) once this value is obtained, it is divided by the 1/750 (-3σ) safety factor to give a value for the required safe-service life, Ar, (cycles). To identify a conservative confidence interval, consider the probability of obtaining a non-finite result at N_i⁻ cycles, given a certain value of the GM (the minus superscript indicates that the value is non-finite).

A 95% lower confidence bound for the true GM can be obtained by identifying that mean value for which the probability of a component not surviving N⁻ cycles is 5%. That is, there is a 95% chance that the defined likelihood lies within the interval 0.05 to 1. Therefore, given the value of N⁻, a 95% lower confidence bound

for GM can be obtained when the following equation is satisfied.

$$p(\text{non-finite at } N^- \text{ cycles}) = 0.05 \quad (3)$$

As the sample size is equal to one, this confidence bound leads to the same formula as would apply if the result were finite. For a sample of size 'n' the confidence test generalises to

$$\prod_{J=1}^n p(\text{non-finite at } N_J^- \text{ cycles}) = 0.05 \quad (4)$$

That is, the probability of obtaining all non-finite results is equal to the product of the probabilities of obtaining the individual non-finite results in the sample. As for a sample of size one, a confidence interval on the GM is chosen such that the probability of obtaining the sample is equal to a value lying between 0.05 and 1. Thus, a conservative 95% lower confidence bound for the GM is given as that value for which this product is equal to 0.05 (see equation 4). This equation embodies a 'next-cycle-failure' assumption for up to one of the non-finite results. It is still slightly overconservative since the probability of even one of the non-finite results reaching dysfunction on its next cycle is extremely low. However, in general, removal of this overconservatism is complex and (without further information) does not result in a significant life increase.

It remains to substitute an expression for the failure distribution into equation 4. First, the change of variable defined by equations 5 and 6 is applied (illustrated in figure 2).

Division by the population geometric mean life, N_μ, then has the effect of placing the origin at the population GM life which has an indeterminate fixed value. N_J⁻ is the resulting non-finite value associated with test result J.

$$N_J^- = \frac{1}{\sigma'_i} \log \left(\frac{N_J^-}{N_\mu} \right) \quad J=1,2,\dots,n \quad (5)$$

$$\sigma'_i = \frac{1}{6} \log \left(\frac{N_{+3\sigma}}{N_{-3\sigma}} \right) \quad (6)$$

The σ' term rescales the axes so that they are in units of standard deviations. N_{+3σ} and N_{-3σ} refer to the ±3σ points on the untransformed distribution. In aeroengine disc lifing, a conservative value of N_{+3σ}/N_{-3σ} = 6 is normally assumed. For a random test result, therefore, the failure distribution in the transformed co-ordinates satisfies the equation

$$P(N' < a) = \int_{-\infty}^a \frac{1}{\sqrt{2\pi}} \cdot \exp\left(-\frac{x^2}{2}\right) dx \quad (7)$$

$$= \text{normal}(a)$$

and substitution of equation 7 into equation 4 gives

$$\prod_{j=1}^n [1 - \text{normal}(N_j^-)] = 0.05 \quad (8)$$

On reversing the change of variable originally applied by equations 5 and 6, the following solution is obtained:

$$\prod_{j=1}^n \left[1 - \text{normal} \left(\frac{\log \left(\frac{N_j^-}{N_\mu^{95\%}} \right)}{\frac{1}{6} \log \left(\frac{N_{+3\sigma}}{N_{-3\sigma}} \right)} \right) \right] = 0.05 \quad (9)$$

where the $N_\mu^{95\%}$ value is a 95% confidence estimate of the GM of the population fatigue life distribution. This is the only unknown in equation 9, and hence can be solved by substitution of the known values and iteration until the equation is satisfied.

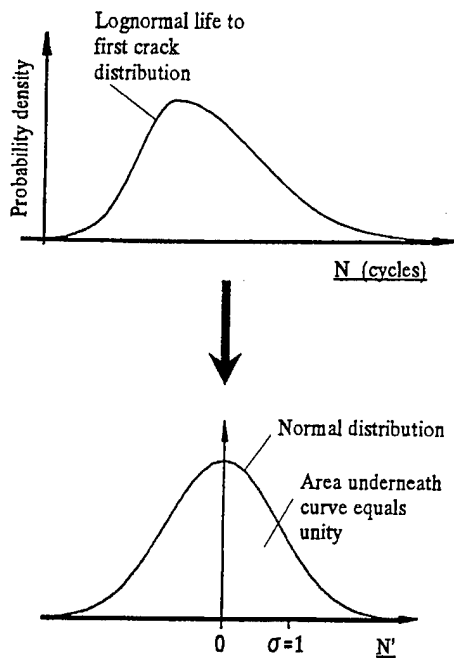


Figure 2. The change of variable from the lognormal to a normal distribution (see equations 5 and 6).

Once $N_\mu^{95\%}$ has been established, the standard safety factor can be applied (as illustrated in equation 2) to ensure that not more than 1/750 components reach the defined dysfunction point. That is,

$$Ar = N_{-3\sigma}^{95\%} = \frac{N_\mu^{95\%}}{\sqrt{\frac{N_{+3\sigma}}{N_{-3\sigma}}}} \quad (10)$$

Returning to the example of 5 non-finite results of 10,000 cycles used in section 4, implementation of equation 9 gives $N_\mu^{95\%} = 10,374$ cycles and substitution of this value in equation 10 gives an Ar value of 4,235 cycles. Thus, in this example and without any compromise to safety, the improved statistical analysis supports a 29% increase in the service life relative to that which could be declared via current regulations. In service, the life extensions given by the method have ranged between 5% and 50%.

2/3 Dysfunction failure criterion

The application of the standard LTFC philosophy does not imply that parts fail immediately the associated crack initiation depth is exceeded. Rather, an acceptable but nonetheless variable margin of safety is given by defining an 'engineering crack' as having a 0.38 mm radius, because the crack radius that gives a constant factor of safety is both geometry and material dependent. This variability is eliminated by replacing the 'engineering crack' life with the life corresponding to 2/3 of the total life to dysfunction⁴. The fraction of 2/3 was selected based on an assessment of a range of disc designs and materials wherein it was found that in most instances, the crack sizes at '2/3 dysfunction' were approximately equal to the 0.38 mm crack radius defined in the LTFC method. Based on the evidence, the 2/3 dysfunction criterion was accepted for general application.

Although service lives are expressed in terms of the major reference cycles experienced, the damage induced by the large number of minor cycles must also be accounted for. Minor cycles occur as a result of adjustments to the thrust requirements during various stages of the mission flown by the aircraft. These are accounted for as the additional number of reference cycles per hour of flight that would inflict equivalent damage to one hour of the minor cycle loading. Then the exchange rate β is defined as the total number of reference cycles (major and minor) consumed during one hour of flight.

Both theoretical analyses and experimental test programmes have shown that, under an identical mission loading sequence, minor cycles are relatively

more damaging during crack propagation than during the LTFC initiation stage. This can be explained in terms of the difference in the 'stress' exponents associated with the life-to-first-crack curve and with the crack growth curve. Below the fatigue endurance limit, minor sub-cycles have virtually no influence on crack initiation, however they can contribute during the propagation phase. During crack initiation (LTFC) the exchange rate ' β_i ' is the average consumption rate of reference cycles per engine flying hour. Whereas ' β_p ' is the average consumption rate of reference cycles per engine flying hour during crack propagation. Thus $\beta_p > \beta_i$. These DERA findings have been confirmed recently for the Tornado RB199 engine for which it has been shown that crack propagation β -factors can be 2-3 times greater than crack initiation β -factors⁵. In this paper, we consider a typical case in which $\beta_p/\beta_i=2.5$.

When LTFC and 2/3 dysfunction lives are equal, the propagation life beyond first crack is another 50% in cycles. However, due to the difference in exchange rate, the crack propagation life amounts to only $\beta_i/\beta_p \times 50\% = 20\%$, in additional hours or actual missions that could be flown prior to dysfunction. This is very significant since the operational management of the fleet is carried out in terms of engine flying hours. Expressing the safety factor, 'S', relative to engine flying hours avoids the direct involvement of both initiation and propagation exchange rate. Hence relative to the mean predicted dysfunction life, at the declared life, 'Ar', the safety factor can be determined from the expression

$$S = 1.2 \times 2.449 \times 6^{\left(\frac{1.645}{6\sqrt{n}}\right)} \quad (11)$$

where the factor of 1.2 is a 2/3 dysfunction safety factor assuming $\beta_p/\beta_i=2.5$. In the current paper, the '2/3 dysfunction' criterion is used to calculate standard 'reference lives' against which life extensions are evaluated.

'2/3 dysfunction crack' tolerant designs

In crack tolerant designs, components have 2/3 dysfunction lives that can be significantly greater than those established via LTFC. The difference represents an additional 'safe crack growth phase' which can be exploited. Assessments of life-limiting areas such as drive arm vent holes and disc rim features have identified some which can exhibit significant crack tolerance. For example, this can occur if the critical area of a component is surrounded by a rapidly decreasing stress field such as at the vent hole of the disc shown in figure 3. The crack growth observed from a similar feature in a RB199 IPC disc is shown schematically in figure 4.

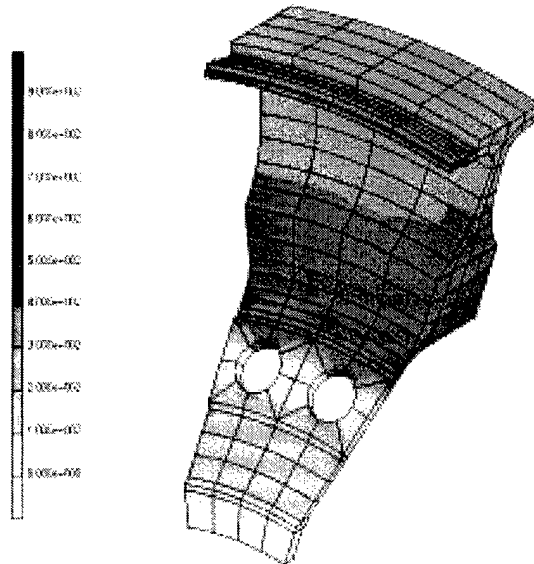


Figure 3. Example of disc with vent holes

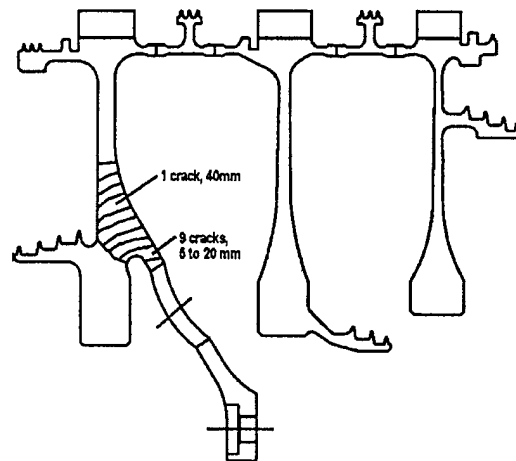


Figure 4. Crack propagation from IPC rotor vent hole.

For such crack tolerant components, service lives can be safely extended beyond 100% Ar, without exceeding the extremely remote risk levels associated with conventional failure locations. However, to ensure a consistent level of safety, the associated 'never exceed' 2/3 dysfunction margin of safety must be imposed on the useable crack growth life. Thus, relative to component lives based on LTFC, life extension is available when the crack growth life is greater than 50% of the LTFC value. To 'cash in' such lives, it is necessary to be able to predict accurately this crack growth phase and hence it is

necessary to apply fracture mechanics procedures based on establishing operating stress intensity levels.

Although life consumption and remnant life calculations are evaluated in terms of reference cycle damage, the end user is interested in the service hours available for specific components. In general to get this information, it is simply a matter of dividing the release lives (in cycles) by the relevant β -factor. The value obtained identifies the authorised service life in engine flying hours. For the situation in which the 2/3 dysfunction life exceeds the LTFC, this difference in reference cycles needs to be divided by the propagation β -factor to establish the authorised additional life in engine flying hours. Extensions of about 40% have been demonstrated for RB199 IPC and IPT rotor components. Details of the procedures involved in determining safe crack growth lives are given elsewhere (AGARD)⁶.

Short term continued use of life expired parts via risk assessment and life management

Situations have arisen in military fleet operation where unforeseen service life reductions have caused in-service engines to include life expired parts. Action has to be taken to replace the parts. The number of life expired parts and the risks would rise rapidly as the fleet-wide profile distribution increases through time. However, to alleviate the situation, it may be possible to 'run-on' such parts for limited periods without significantly affecting the overall risk.

As formulated, current lifeing procedures are used directly to estimate risk because they apply 'safety factors' which mask the true risk. To assess the risks of disc failure, the applied safety factors need to be replaced by statistical modelling of the sources of component life uncertainty. This section of the paper addresses the core of the risk assessment model. Although the air authorities are interested in the overall risks experienced by the fleet, in practice, the focal issue is usually the additional risks incurred as a consequence of operating individual components beyond their declared life, A_r . The initial stage in the assessment therefore quantifies the safety factors associated with A_r . The combined safety factor S associated with the mean dysfunction life A_r can be determined in engine flying hours from equation 2 and is given by the equation:

$$S = 1.2 \times 2.449 \times 6^{\left(\frac{1.645}{6\sqrt{n}}\right)} \times \left(\frac{A_r}{H \times \beta_i}\right) \quad (12)$$

where H is the component life in hours. To simplify the derivation, the fatigue results and the safety factors are transformed to normal distribution functions. The

risk per engine flying hour is defined as the rate of increase of probability of failure with respect to increased engine flying hours.

$$risk / efh = \frac{\partial\{p(fail)\}}{\partial H} \quad (13)$$

Since it is easier to consider the risk in terms of the rate of increase of the transformed variable $\delta S'$ (i.e. $\log S$), the following partial derivative is used:

$$risk / efh = \frac{\partial\{p(fail)\}}{\partial S'} \times \frac{\partial S'}{\partial H} = - \frac{\partial\{p(fail)\}}{\partial S'} \cdot \frac{1}{H} \quad (14)$$

Given an infinite sample of component test results, there would be no sampling error. This artificial case can be used to illustrate the principle of the risk model. In this case, the location of the component life relative to the GM of the burst distribution would be precisely determined as shown in figure 5. Therefore, the risk/efh is simply equal to the shaded area in the figure.

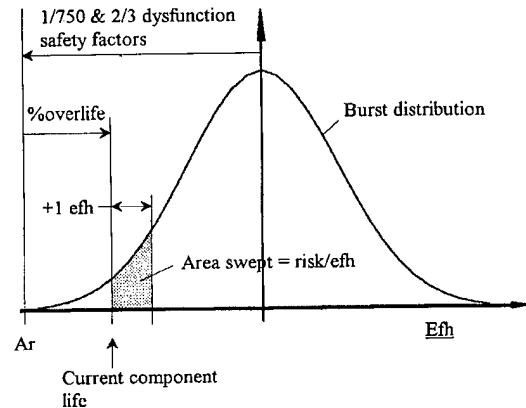


Figure 5. Illustration of the risk assessment model for the case where the geometric mean of the population burst distribution is known.

In lifeing procedures for fracture critical components, both the form and the scatter of the population burst distribution are assumed to be identified. A consequence of these assumptions is that, given a (known) failure distribution of an infinite population, each result can be considered as the mean of a sample of one. If groups of samples of 2, 3, 4... n are randomly selected from the total population, the means of the individual samples of size 'n' will also have a known distribution. Hence, a single component test sample of size 'n' will have a known error band associated with

its use in the estimation of the mean of the total population. This is particularly important in risk analysis since the location of the population mean solely from the mean of the sample and without consideration of sampling error can lead to an underprediction of the 'best estimate' of the risks associated with individual service components. The sampling error x' , is equal to the difference between the sample GM and the population GM. In other words, the location of a component service life relative to the burst distribution is not precisely identified. Equally, and in practice, the analysis can be considered from the viewpoint of an error in the service component life location relative to the burst distribution, as illustrated by figure 6.

It follows that for a specified location of sampling error, x' , the risk/efh is equal to the integral of the probability of burst distribution over the interval (efh) to (efh+1). The total risk/efh is now the summation, or the integral of these risks multiplied by the probability that the sampling error is x' . Hence, to account for the sampling error x' , the risk/efh is equal to the integral of the risk/efh given the location x' of the sample mean on the sampling distribution times the probability of the sample mean being located at x' on the sampling distribution. Since the probability density function for

the sampling error x' can be determined, then the following standard statistical equation can be used to solve the risk /efh.

$$P(y) = \int_{-\infty}^{\infty} P(y | x') \cdot PD(x') \cdot \partial x' \quad (15)$$

where 'y' is the risk/efh. The solving of the above equations to give an expression in terms of risk levels associated with individual life expired discs is explained elsewhere⁶. Equation 16 is the basic form of this solution and is used in some current risk assessments.

(16)

$$\frac{\partial(\text{risk})}{\partial(H)} = \frac{1.5}{H} \sqrt{\frac{n}{n+1.239}} \times \exp \left[-6.949 \left(\frac{n}{n+1.239} \right) \left(\ln \left(\frac{H}{Ar \times \beta_1} \right) - 1.0782 - \frac{0.49094}{\sqrt{n}} \right)^2 \right]$$

'H' is the life of the component in efh and 'n' is the size of the component test sample.

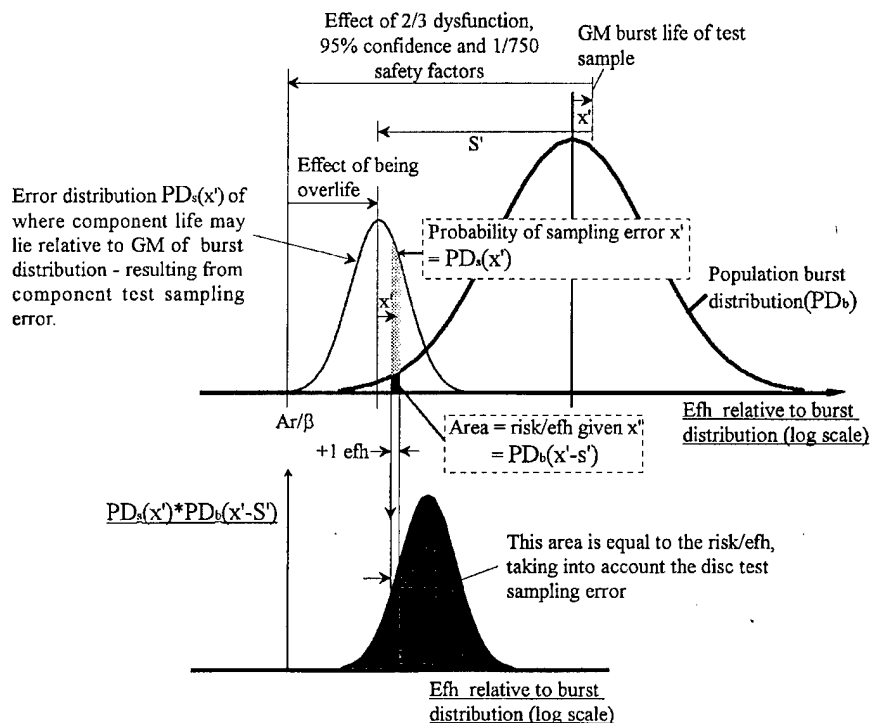


Figure 6. Illustration of the incorporation of disc sampling error into risk assessment.

In the example of a component with a declared safe service life of 10,000 cycles, calculated from a test sample of 3, and for a cyclic exchange rate of 2.0, at full Ar, substitution into equation 20 gives an estimated risk/efh of 2.8×10^{-8} . If the declared safe service life of the component were required to be reduced by 20% to 8,000 cycles, then at a life of 10,000 cycles, such a component would incur a risk of 2.1×10^{-7} /efh. Thus, for an individual disc close to the old service life, if this risk level is deemed acceptable, then such a service life could be maintained for a limited period whilst replacement parts are procured.

The form of results obtained from a risk analysis of a typical aeroengine component, in this case for an HP turbine disc, with safe service life Ar=5,201 cycles are illustrated in the following two tables. Table 1 provides the calculated risk per efh at the service life for the component. In addition, it provides estimates of the 'available' additional service until the operating risks reach the levels defined at the foot of the respective columns.

Total cycles	5,201	5,344	5,828	6,464
Cycles over Ar	0	143	627	1263
Efh over Ar	0	44	194	391
Risk/efh /engine	7×10^{-8}	1×10^{-7}	3×10^{-7}	1×10^{-6}

Table 1 Estimated lives corresponding to specified risk level/efh/engine using a spin test sample size of 5, where β_1 equals 3.23. Propagation exchange rates are assumed to be 2.5 times those for initiation.

Service Interval (efh)	Additional risk/efh/engine				
	From 3×10^{-8} to 10^{-7}	From 10^{-7} to 3×10^{-7}	From 3×10^{-7} to 10^{-6}	From 10^{-6} to 3×10^{-6}	Greater than 3×10^{-6}
0	7	1	-	-	-
50	10	3	-	-	-
100	8	5	1	-	-
150	9	9	1	-	-
200	11	10	3	-	-
250	13	10	6	-	-
300	18	9	9	1	-

Table 2 Estimated numbers of discs falling within the specified risk bands during each additional 50 hour service interval

Table 2 provides an estimate of the number of engines currently in each risk band and, assuming historic fleet usage, how this changes during the next 50 hours and subsequent 50 hour service intervals. The table assumes no action by the control authority to replace high risk parts, but provides the information needed to estimate the minimum rates of component replacement to ensure that specific risk levels are not exceeded.

Lifing using microstructural models

Current lifing regulations do not permit read across of fatigue lives from one component geometry to another, even assuming there are similarities, of material, surface finish, etc. This limitation adds considerably to the numbers of component tests required in aeroengine developments. Further, although disc testing experience shows that the assumption that the forged disc LCF life scatter factor $sf=6$ is conservative, the value of 6 may in some cases be over conservative given additional information. To overcome these limitations will require microstructural modelling aspects to be addressed such as the following.

i) Modelling the defect failure mechanism

Component lives are affected by the type and distribution of defects present. These distributions can be accounted for probabilistically. In addition, following cracking of a significant defect, a number of fatigue cycles is necessary to develop a slip band and crack in the surrounding matrix (referred to as the incubation period).

ii) Modelling the effect of the critical-area volume

The volumes of the critical areas of a component can have a significant effect on its life. It can be shown that the probability of a fatigue crack of a specified small size forming at a life N in a volume V of material uniformly loaded to a constant load cycle $\Delta\sigma$ is given by the expression

$$F[N;V] = 1 - e^{-g[N]V} \quad (17)$$

where $g[N]$ can be measured by experiment. Assuming that the function g is derived experimentally from a failure distribution $F[N;V_0]$ for specimens with critical area volume V_0 , the following expression is obtained.

$$F[N;V] = 1 - (1 - F[N;V_0])^{V/V_0} \quad (18)$$

A current DERA research activity is to develop the theory to allow the volume effect to be accounted for in lifing predictions. In models under development the Weibull or lognormal forms of the function F are being explored.

iii) Accounting for fabrication process variability

Fabrication process variability can contribute significantly to scatter in component life. For example, if the uts of the material varies by up to a factor of 1.3 and the exponent of the SN curve for the material is 5.28, then the effect of this variability on the life capability of the material is a factor of about $1.3^{5.28} = 4$ in life. Any method that can be found to reduce deviations of processing from the optimum could enable the scatter in component lives to be reduced, and in theory this could enable longer safe service lives to be declared for the component.

iv) Short crack growth modelling

In addition to the LCF life associated with defect cracking, part of a 2/3 dysfunction life consists of short crack growth. The following sections in this paper describe a short crack growth model which is capable of making some useful lifing predictions. These sections describe the experimental method, explain how the short crack fatigue data was analysed, briefly explain the model and present some results.

Experimental

Bar specimens were cut from a disc forging of Waspaloy having a nominal chemical composition of 57% Ni, 19.5% Cr, 13.5% Co, 4.3% Mo, 3% Ti, 2% Fe, 1.4% Al, 0.09% Zr, 0.07% C and 0.006% B.

The specimens were loaded in four point bend and fatigue cycled at 20°C as follows. Semicircular short cracks were initiated in the specimens without notches at $R = \sigma_{\min} / \sigma_{\max} = 0.1$, $\sigma_{\max} = 880\text{MPa}$ and were grown to a surface length (2a) of 150µm. In a long crack specimen, a pre-crack was grown to a depth of 3mm beyond a sharp through-notch. After pre-cracking, the stress ratio R was increased to 0.5 and all cracks were grown beyond the old plastic zone, so that subsequent fatigue was undisturbed by the prior load history.

The fatigue cracks were grown at $\Delta K = 4.5\text{-}7\text{ MNm}^{3/2}$ to characterise the short crack regime, at $\Delta K = 12\text{-}12.5\text{MPa}\cdot\text{m}^{0.5}$ to characterise the short-to-long crack growth transition and $\Delta K = 18.7\text{-}19.5\text{ MNm}^{3/2}$ to characterise the long crack regime. That is, σ_{\max} was set at 880MPa so ΔK increased as the cracks grew, and the detailed measurements were taken in the three ΔK intervals stated above. The two surface radii of the short cracks (measuring from the centre of the initiation site) were measured at the respective cyclic intervals of 2000, 250 and 20 cycles. The long crack was grown at $\Delta K = 12\text{-}12.5\text{ MNm}^{3/2}$ and at just above ΔK_{th} (near threshold). Long crack depth measurements were read from either side of the specimen every 250 elapsed cycles (and every 2,000 cycles near threshold). These cyclic intervals were specifically chosen to give an average crack extension between measurements of about 1/40th of a grain width, that is, 0.5µm. Within each

analytical ΔK interval, the test was continued for 200 measurement intervals.

Analysis of short crack growth data

Crack growth at an observable point on a surface-crack front was measured over uniform cyclic intervals to a resolution of 0.2µm. On this basis, the rate of crack growth over an individual interval of cycles is either positive (growing) or zero (arrested). These two states of observed crack activity are mutually exclusive.

The crack growth rate curve was then cut into sections. Each section corresponds to a single measurement interval (ie. 20, 250 or 2,000 cycles), during which there occurred crack growth or part of an arrest (that spans one or more intervals). Those sections associated with crack growth are put into one sample and those associated with crack arrest are put into a second sample. The two samples are analysed separately as follows.

For arrests, the persistence in cycles of each identified arrest event is counted. A histogram was then plotted of frequency versus persistence of arrest and examples of the results are shown in figures 7a1&2. (Arrest persistences depend on ΔK and therefore the ideal would have been to obtain crack growth data at constant ΔK . In practice, the measurements were taken over three narrow ΔK bands. An algorithm was developed to correct these distributions, so they apply for iso- ΔK , however, in these 3 examples the corrections were relatively small). A detailed analysis of these results is provided elsewhere⁷.

In every case, it was found that during crack growth the rates of crack growth during consecutive measurement intervals of cycles were independent, irrespective of the loading conditions, crack geometry and crack size. It follows that the entire fatigue process can be broken down into small increments of time that are independent. Also, owing to crack arrest at points along the crack front, the activity the crack front can be considered as a chain of independently growing sections. These two attributes can be used to simplify considerably the modelling of the microstructural mechanism of fatigue crack growth.

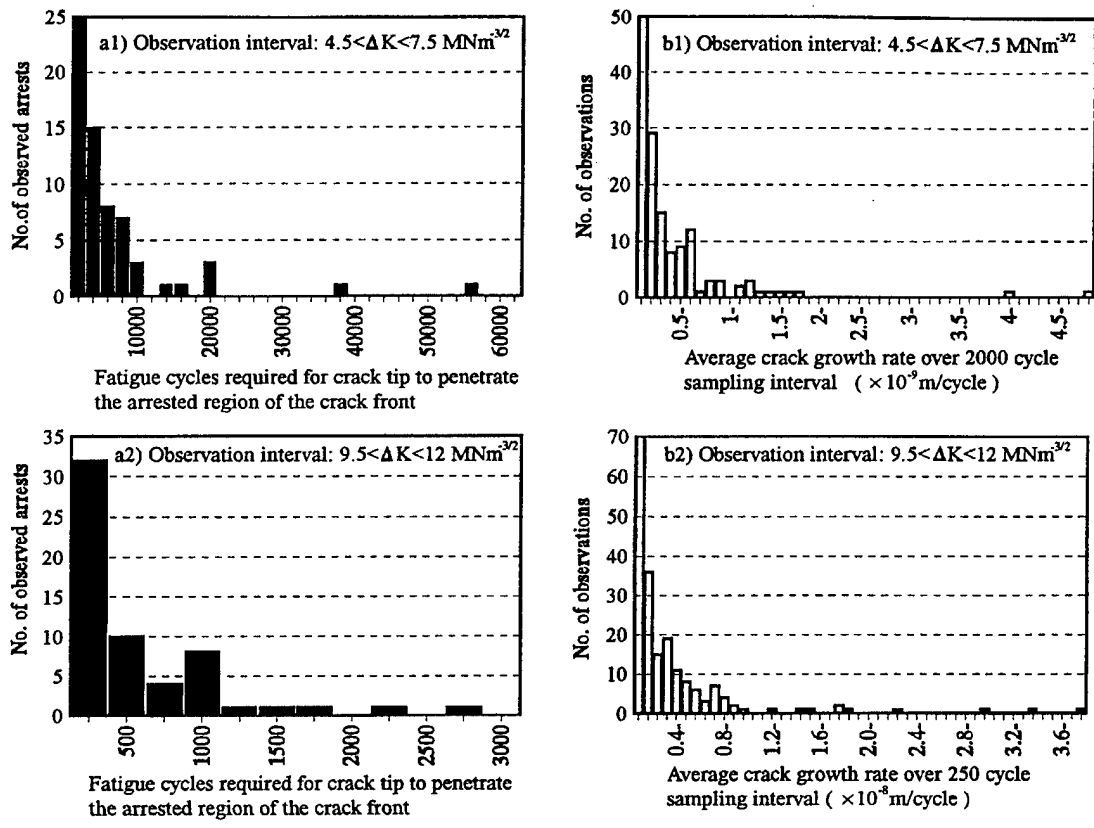


Figure 7. Examples of discrete statistical analyses of persistences of crack arrest and of instantaneous crack growth rates, for $R=0.5$.

Short crack growth lifing model

The above experimental observations can be used as input to the following Monté Carlo model of the microstructural mechanism of fatigue which is capable of making fatigue lifing predictions. At time zero, the model represents an infinite population of small cracks, present in an infinite sample of components. For simplicity, consider the hypothetical case where, at time zero all of the cracks have a radius of $100\mu\text{m}$. As in the experimental method, crack size is characterised by a single measurement of the centre point of the crack initiation site to a defined point on the crack front. Time is then advanced in constant steps of fatigue cycles.

For those cracks that are arrested, the arrest distribution as a function of ΔK is used to decide how long each arrest will last for (derived from results such a shown in figures 7a1,2). The probability that an individual crack grows a distance 'x' during a time step is given by the probability density versus instantaneous crack growth rate relationship for the particular value of ΔK . Also, the model uses the probability of a growing crack front becoming arrested, which is similarly an experimentally determined function of ΔK . Further details of the method are reported elsewhere⁷.

The predictions of the model can be plotted as probability vs. crack length vs. life diagram. For the case considered where all cracks start at an initial length

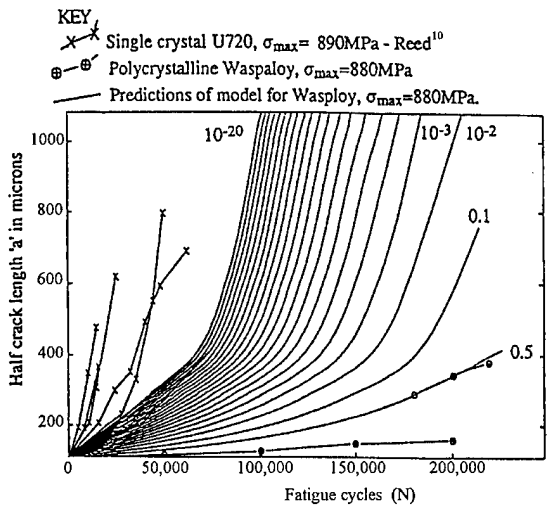


Figure 8. Example prediction of short crack model. of $100\mu\text{m}$, the prediction of the model is shown in figure 8. The smooth line labelled 0.5 is the predicted median

line. The predicted line labelled 0.1 represents the 0.1 probability quantile, etc.

The model predicts that LCF crack propagation lives are distributed according to a lognormal distribution to a good approximation. This result agrees with detailed experimental studies of distributions of crack propagation lives in some other polycrystalline metals as well as of the Ni-base superalloys⁸.

Using arrest and instantaneous crack growth data for near threshold, the model also predicts that HCF lives are distributed according to a lognormal distribution to a good approximation. This is a significant prediction, since the typically large scatter in HCF lives (in cycles), prohibits the determination of this result directly by experiment.

In its present form, the model under predicts the scatter factor 'sf' for a crack propagation life. A value of sf=2 is obtained, whereas experimental evidence shows⁴ that to be conservative a value of 4 must currently be assumed. This is not surprising, since the experimental data inputted to the model came from a very small sample of microstructure. It is anticipated that if the effect of fabrication process variability were included then a higher value closer to 4 would be obtained.

Conclusions

- 1) Life extension of fracture critical parts beyond the values given by the standard LTFC method is sometimes possible.
 - 2) Exploitation of non-finite fatigue test results can give safe life extensions of between 5% and 60% (in efh). The benefit is an increasing function with respect to both the number and significance of the non-finite results in the sample.
 - 3) Exploitation of the full safe-service-life capability of crack-tolerant components can give safe life increases of up to 50% (in efh) over those associated with conventional safe life procedures.
 - 4) Care is required to define the procedures by which new safe life extension capabilities can be safely implemented in a form that minimises scope for error.
 - 5) Limited service operation to lives beyond Ar may be possible with little compromise of safety. The life increase available is dependent on the level of risk deemed acceptable in the circumstances. The risk model developed in the paper illustrates that life increases of up to 20% may be possible at the cost of less than an order-of-magnitude increase in the risk/efh.
- 6) Results from a statistical model of short crack growth are presented. Reduction of fabrication process variability could theoretically reduce component life scatter and thus enable longer component lives to be declared

References

1. UK Military Defence Standards, Def. Stan 00-971, General Specification for Aircraft Gas Turbine Engines, 1986.
2. Joint (European) Airworthiness Requirements - Engines (JAR-E), Civil Aviation Authority, 1986.
3. 'Mechanical Survival', J.H. Bompas-Smith, pub. McGraw-Hill, Maidenhead, England, 1973.
4. 'Life assessment of fracture critical aeroengine parts', G. F. Harrison, Int Conf. Sheffield 1997.
5. 'Critical parts life extension based on Fracture Mechanics', P. Blüml and J. Broede, RTO Workshop 'Qualification of Life Extension Schemes for Engine Components, Oct 1998.
6. 'The development of life extension methods for fracture-critical aeroengine components', A. D. Boyd-Lee and G. F. Harrison, RTO meeting proceedings, NATO, RTO-MP-17, 18-1, 5-6 Oct. 1998.
7. 'Fatigue crack growth resistant microstructures in polycrystalline Ni-base superalloys for aeroengines', A.D.Boyd-Lee, Int. J.Fatigue, Vol. 21, No.4,1999, pp393-405.
8. 'Discrete statistical model of fatigue crack growth in a Ni-base superalloy capable of life prediction', A.D.Boyd-Lee and J.E.King, Fatigue Design ESIS 16 (Edited by J.Solin et.al.), 1993, Mechanical Engineering Publications, pp283-296.
9. 'Bootstrap analysis of FCGR, application to the Paris relationship and lifetime prediction', M.Bigerelle and A.Iost, Int. J. Fatigue, Vol. 21, No.4, 1999, pp299-307.
10. 'Comparison of long and short crack growth in polycrystalline and single crystal Ni-based alloy Udimet 720', P.A.S. Reed and J.E.King, Paper 5, Proc. Short Crack Conference, University of Sheffield, Dec 1990.